SEISMIC BEHAVIOUR OF HIGH-STRENGTH-STEEL MRFS EQUIPPED WITH SELF-CENTRING ENERGY DISSIPATION BAYS

K. Ke[(1) (2)], HY. Zhang[(2)], XH. Zhou[(1) (2)], MCH. Yam[(3) (4)], YW. Li [(3)]

[(1)] Key Laboratory of New Technology for Construction of Cities in Mountain Area, School of Civil Engineering, Chongqing University, Chongqing, China
Emails: keke@outlook.com;keke@hnu.edu.cn
[(2)] Hunan Provincial Key Laboratory for Damage Diagnosis of Engineering Structures, Hunan University, Changsha, China
[(3)] Department of Building and Real Estate, The Hong Kong Polytechnic University, Hong Kong, China
[(4)] Chinese National Engineering Research Centre for Steel Construction (Hong Kong Branch), The Hong Kong Polytechnic University, Hong Kong, China

Abstract

The high strength steel (HSS) moment resisting frames with energy dissipation bays (EDBs) were proved to have good seismic behaviour and encouraging damage evolution mode. In this paper, the moderate energy dissipation capacity and self-centring characteristics of the super-elastic SMA bolts were applied in the energy dissipation bay to form HSS moment-resisting frames equipped with self-centring energy dissipation bays (HSSF-SCEDBs). Then, a prototype HSSF-SCEDBs structure was preliminarily designed according to Chinese seismic design provisions, and the focus of the current study was given to a 2-D frame. For the prototype building, HSS with the yield strength of 460 MPa was used to develop the main frames. Two self-centring energy dissipation bays (SCEDBs) were located at the external bays of the structures, and connections equipped with the super-elastic SMA bolts were installed in the SCEDBs. To concentrate the inelastic actions in the SCEDBs, simple connections were utilised to connect the SCEDBs with the main frames. For further analysis of HSSF-SCEDBs, both nonlinear static procedures (pushover analysis) and nonlinear response history analysis (NL-RHA) based on experimentally verified numerical models were performed, and the P-Δ effect was considered. The cyclic pushover response of the prototype structure shows that HSSF-SCEDBs exhibited damage-control behaviour for a wide inelastic deformation range and the insignificant residual drift in the damage-control stage. Also, good agreement between the cyclic pushover responses and the flag-shape idealisation was observed in a wide deformation range. With the increase of the loading drift, stiffness hardening was also observed due to material properties of SMAs (i.e. Martensite hardening). In the NL-RHA, twenty ground motions are selected from the SAC project (i.e. coded from LA01 to LA20) as excitations to analyses of the prototype structure. According to the database of NL-RHAs, it was found that the mean values of the maximum inter-storey drift were usually uniform distributed along with the building height (despite the first storey). The dispersion quantities of the interstorey drift ratios over the building height fall in a reasonable range. The post-residual story drift (the drifts extracted after 100 s of oscillation following the input earthquake) were insignificant, and the potential of the concept of the HSSF-SCEDB was seen. Thus, the encouraging post-earthquake residual deformation of an HSSF-SCEDBs are confirmed. The ratio of plastic energy dissipation of the main frames and the entire structure under ground motions show that SCEDBs were the primary source of hysteretic energy dissipation, and the main frames are slightly damaged even damage-free in the expected deformation range. In summary, HSSF-SCEDBs is promising in contributing to further enhancing the seismic performance of an HSSF-EDBs, and this study also provides a new idea for the application of SMA bolted beam-column joints in a structure.

Keywords: high strength steel, Self-centring, Energy dissipation bay, nonlinear response history analysis.

1. Introduction

Steel moment-resisting frames (MRFs) are extensively used for low-to-medium rise building structures. To ensure that the life-safety objective is achieved, MRFs are usually designed to experience large inelastic deformation to dissipate the energy of the input strong earthquakes [1]. However, recent earthquake attacks exposed deficiencies of conventional MRFs which underwent large inelastic deformations. These large inelastic deformations can result in substaintial post-earthquake residual drifts [2]. Thus, researchers have developed innovative MRFs to achieve improved seismic behaviour. For example, innovative steel MRFs equipped with various energy dissipation components were investigated. Ke and colleagues [3-6] have explored the effectiveness of energy dissipation bays for enhancing the seismic behaviour of a high strength steels (HSS) frame. The enhanced seismic behaviour of the structure was verified by experimental investigations [3,4]. It is worth noting that the post-earthquake residual drift is a critical index to determine whether a building should be repaired or demolished. McCormick's research [7] showed that if the post-earthquake residual interstorey drifts of the structure exceed 0.5%, the structure may need to be demolished. Therefore, it is of great significance to mitigate the post-earthquake residual deformation of a structure, and applying the "self-centring technology" based on post-tensioning connections or Shape Memory Alloys (SMA) [7-9] in steel MRFs becomes a promising solution.

In light of the above, this study explores the seismic behaviour of an innovative structure, i.e. steel MRFs with HSS members and self-centring energy dissipation bays, namely the HSSF-SCEDB structure. In particular, it is proposed that smart connections equipped with Shape Memory Alloy are installed in the self-centring energy dissipation bays (SCEDBs), and SCEDBs may dissipate energy and realise excenllent self-centring behaviour. The primary objective of this conference paper is to explore the seismic behaviour of HSSF-SCEDB structure. The seismic behaviour of a prototype HSSF-SCEDB is examined by cyclic pushover analysis and nonlinear response history analyses (NL-RHAs). The critical engineering demand indexes such as maximum interstorey drift (MID), post-earthquake residual interstorey drifts (RID), plastic energy dissipation and peak absolute floor acceleration (PA) are gathered from the analysis database and examined in detail.

2. Prototype buildings

2.1 Basic information about the prototype structure

To explore the seismic behaviour of the HSSF-SCEDB system, a proof-of-concept study is initiated recently. The basic information about the prototype structure is shown in this section. The prototype structure includes three-stories and four-bays. The three-storey prototype structure is designed according to the Chinese seismic design provisions [10]. The structure is designed as an office building and located on sites with stiff soil. This focus of the current conference paper study is the 2-D frame that represents the east-west (EW) direction of the structure. In the EW direction, the HSSF-SCEDB is composed of four bays, including two HSS main frames and two SCEDB bays, as shown in Fig. 1. Two self-centring energy dissipation bays (SCEDBs) are located at the external bays of the structures, and the SMA connections are installed in the SCEDBs. The column bases are fixed. In the horizontal direction, the dimension of the self-centring energy dissipation bays and the HSS frame is 1.5 m along with 6.0 m, respectively. A SCEDB is composed of two HSS columns and beams connecting the columns, and self-centring connections with the super-elastic SMA bolts are used to connect the beams with the columns (Fig. 1b).

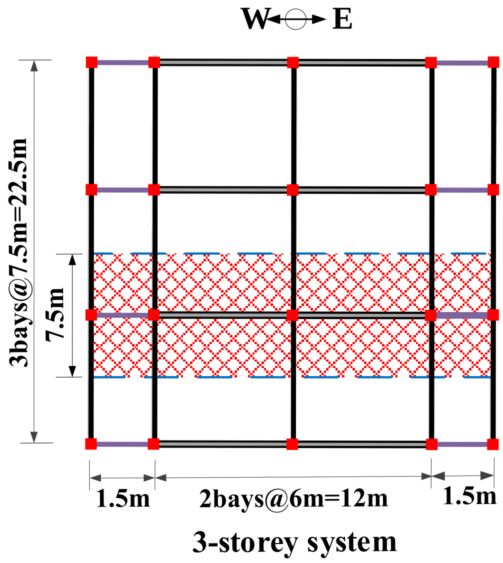

(a)

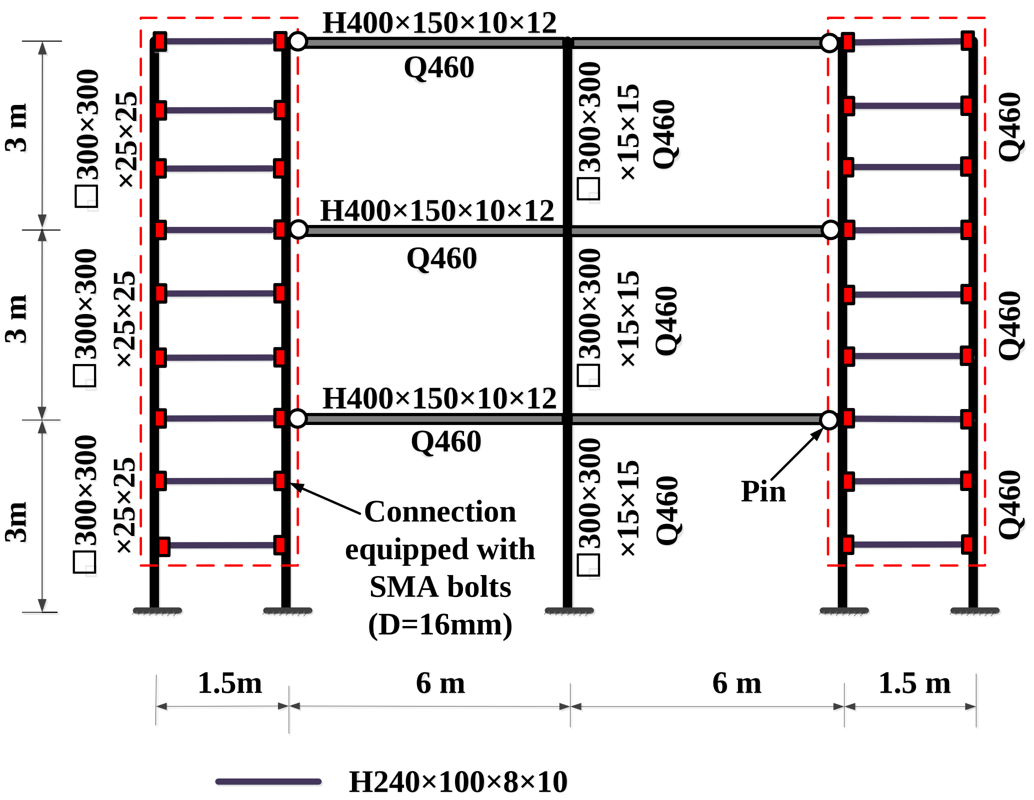

(b)

Fig. 1 – Structural arrangement of prototype systems: (a) structural layout, (b) 3-storey system.

The elastic seismic demand for the prototype structure is determined based on design spectra documented in GB50011-2010 (2016) [10]. For the prototype structure, according to the Chinese load code for the design of building structures (GB5009-2012) [11], it is assumed that the dead load of 5 kN/m^2 and the live load of 2.5 kN/m^2. The seismic weight and gravity load are calculated from the tributary area as shown in Fig. 1. The modelling techniques will be discussed in later sections.

2.2 Finite element modelling techniques of the prototype structure

The prototype structure is modelled in the finite element (FE) software ABAQUS [12]. The columns and the beams of the model are modelled using the two-node linear beam elements, i.e. B31 elements, in ABAQUS nomenclature. The mesh size for the area away from the plastic hinge of the member is set as 200 mm, while the mesh size of the area expected to experience significant inelastic action is set as 50 mm. The rigid joint assumption is applied to the connections in the main frames. The "Release" option [12] is used to simulate the pin connections in the structures (Fig. 1). For steel material, the bilinear kinematic hysteretic material model with von Mises yield criterion is used, the nominal yield strength of the prototype structure members (i.e. beams and columns) is 460 MPa. As for the SMA, the Auricchio's material model [13] is adopted to simulate the behaviour of the superelastic SMA bolts. The essential material parameters including forward transformation start stress (σ^{MS}), forward transformation end stress (σ^{Mf}), reverse transformation start stress (σ^{AS}) and reverse transformation end stress (σ^{Af}), austenite elasticity (E^{A}), martensite elasticity (E^{M}), maximum transformation strain (ε^{L}), and poisson ratios (v^{A} and v^{M}), are based on Fang et al. [14] as shown in Fig. 2 and Table 1.

Table 1 – SMA material properties used in the FE study [14].

Material properties	Values
Forward transformation start stress σ^{MS}	280 MPa
Forward transformation end stress σ^{Mf}	380 MPa
Reverse transformation start stress σ^{AS}	150 MPa
Reverse transformation end stress σ^{Af}	75 MPa
Austenite elasticity E^{A}	35 GPa
Martensite elasticity E^{M}	25 GPa
Maximum transformation strain ε^{L}	5%
Poisson's Ratio v^{A}	0.33
Poisson's Ratio v^{M}	0.33

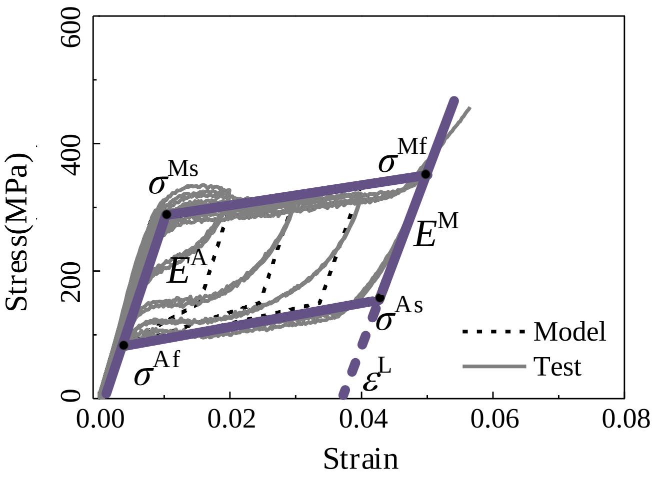

Fig. 2 – Material properties of SMA bars [14].

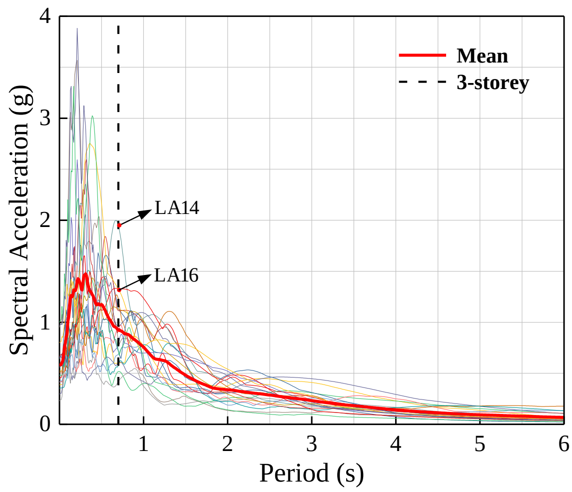

Fig. 3 – Acceleration spectra of earthquake motions.

3. Seismic response of prototype structures

3.1 Analysis procedures

To explore the seismic behaviour of the HSSF-SCEDB system, both nonlinear static procedures (pushover analysis) and nonlinear response history analysis (NL-RHA) are performed, and the P-Δ effect is considered. The cyclic pushover analysis is achieved by using the invariant lateral force pattern corresponding to the fundamental vibration mode. In order to obtain the lateral load vector, the frequency analysis should be carried out first. Table 2 shows the elastic dynamic properties of the prototype structure. "Equation" option in ABAQUS [12] is used to apply the invariant lateral load distribution.

The NL-RHAs are applied to examining the seismic response of prototype structure subjected to the ground motions. In this study, twenty ground motions are selected from the SAC project (i.e. coded from LA01 to LA20) as excitations to analyses of the prototype structure [15]. They are recorded as ground motions on sites of stiff soil with 10% probability of exceedance in fifty (50) years. Fig. 3 shows the acceleration spectra with the damping ratio at 5%. In NL-RHAs, a damping ratio of 5% [16] is used to develop the Rayleigh damping matrix for the first two vibration modes. To capture the residual interstorey drift responses of the prototype structure after a ground motion, additional analysis time (100s) were added following the input earthquake.

Table 2 – Dynamic properties of the prototype HSSF-SCEDBs.

Structure	Property (unit)	1st Mode	2nd.Mode
3-storey system	Period (s)	0.70	0.17
	Modal effective mass (t)	179.54	19.22
	Modal participation factor	1.30	0.50
6-storey system (A) (L_{SMA}=75 mm)	Period (s)	1.67	0.54
	Modal effective mass (t)	466.10	77.20
	Modal participation factor	1.37	0.53
6-storey system (B) (L_{SMA}=150 mm)	Period (s)	1.90	0.62
	Modal effective mass (t)	469.21	71.99
	Modal participation factor	1.36	0.52

3.2 Case study and cyclic pushover responses

The seismic behaviour of HSSF-SCEDB under a ground motion (LA08) is examined through a case study. The displacement (u_g), velocity (v_g) and acceleration (a_g) time-history responses of the ground motion (LA08) are shown in Fig. 4. It is found that the ground motion has large acceleration and velocity pulses but with insignificant permanent displacement, and the dominant pulse occurs at 15-20s.

Fig. 5 shows the responses of the interstorey drift and absolute floor acceleration of each floor of the prototype structure under the ground motion (LA08). Each floor of the prototype structure generally exhibits a similar peak interstorey drift and absolute floor acceleration, which occurs at the dominant seismic velocity pulse (i.e. 15-20s). As shown in Fig. 5a, after undergoing peak interstorey drift, the prototype structure immediately rebounded with a smaller reverse peak interstorey drift, which is due to the unique flag-shaped hysteretic responses of the HSSF-SCEDB. In addition, each floor of the prototype structure oscillates near the zero-drift line with the insignificant interstorey residual drifts. Fig. 5b shows the responses of the absolute floor acceleration of the prototype structure. The prototype structure shows large absolute acceleration response, the peak absolute acceleration value achieves 0.75g, which is almost twice as much as the PGA (0.42g). Thus, the HSSF-SCEDB structure may significantly amplify the ground acceleration, and may cause economic losses associated with the damage to the non-structural component.

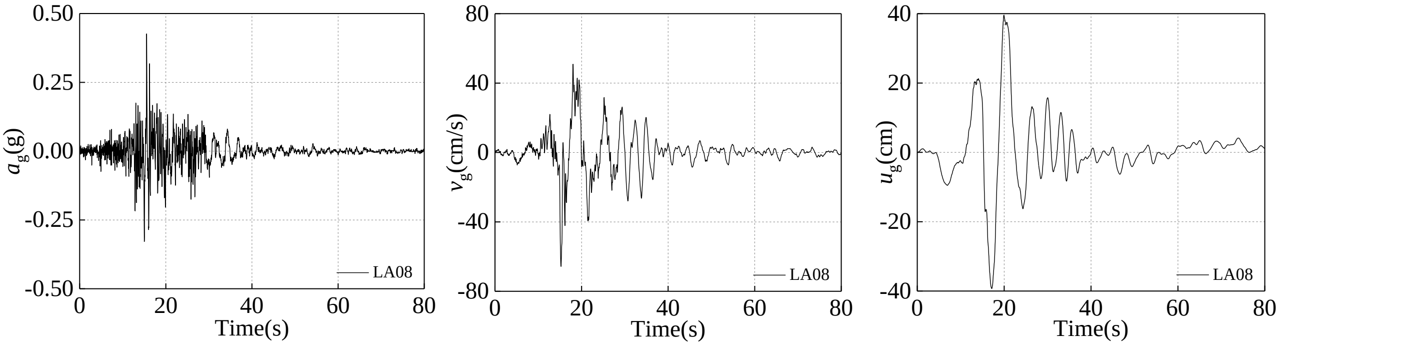

Fig. 4 – Time-history responses of the ground motions (LA08).

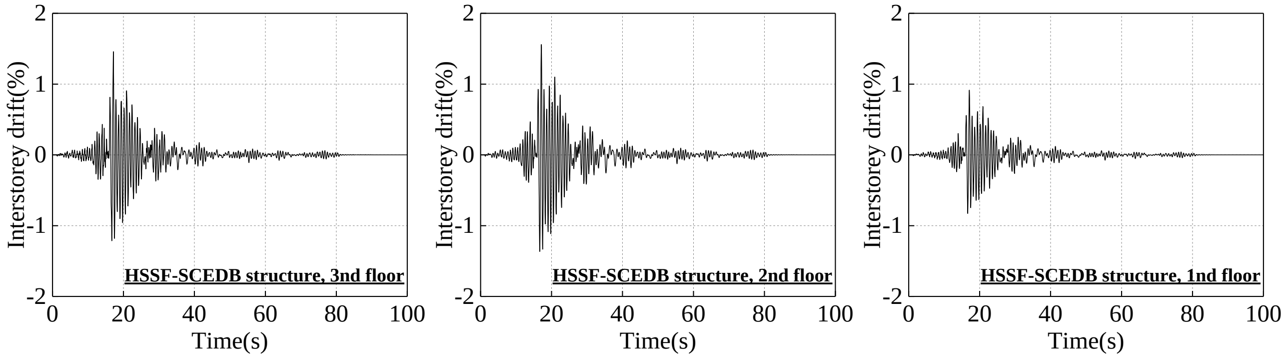

(a)

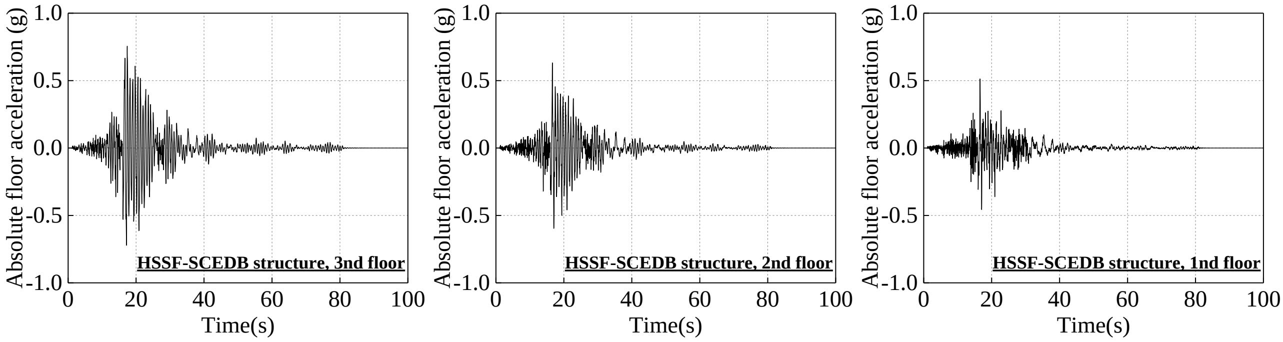

(b)

Fig. 5 – Case study: (a) interstorey drift responses, (b) acceleration responses.

The cyclic pushover response of the prototype structure (up to the maximum roof drift of 4%) is shown in Fig. 6. The cyclic pushover response of the prototype structure shows a typical flag-shape hysteretic response, excellent self-centring behaviour and good energy dissipation capacity. With the increase of the loading drift, stiffness hardening is also observed due to material properties of SMAs (i.e. Martensite hardening).

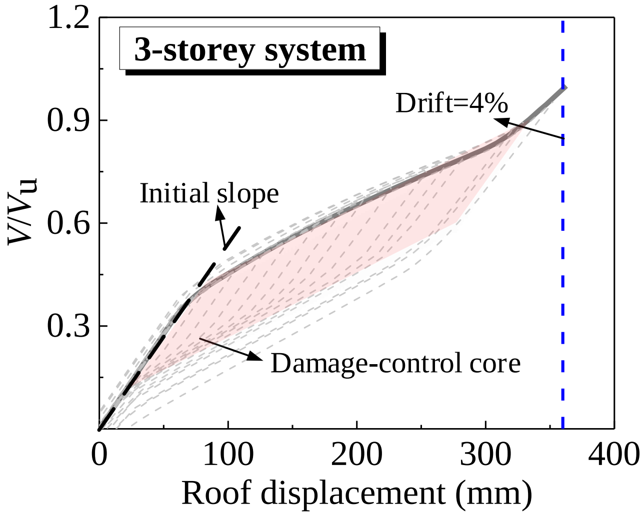

Fig. 6 – Cyclic pushover response of prototype structures.

3.3 Seismic response of prototype structure under ground motions

Fig. 7 shows the responses of the maximum interstorey drifts (MID), residual interstorey drifts (RID) and peak absolute floor acceleration (PA) of the prototype structure under each individual ground motion. The median, mean and 84th percentile values of the demand indexes are also illustrated. The prototype structure undergoes the most intense earthquake responses when subjected to ground motion LA14 and LA16. According to Fig. 3, At the first mode period of the prototype structure (i.e 0.7s), the two ground motions (LA14 and LA16) have the most significant spectral accelerations. Thus, it appears that the deformation responses of the prototype structure are associated with the spectral acceleration of the first mode period.

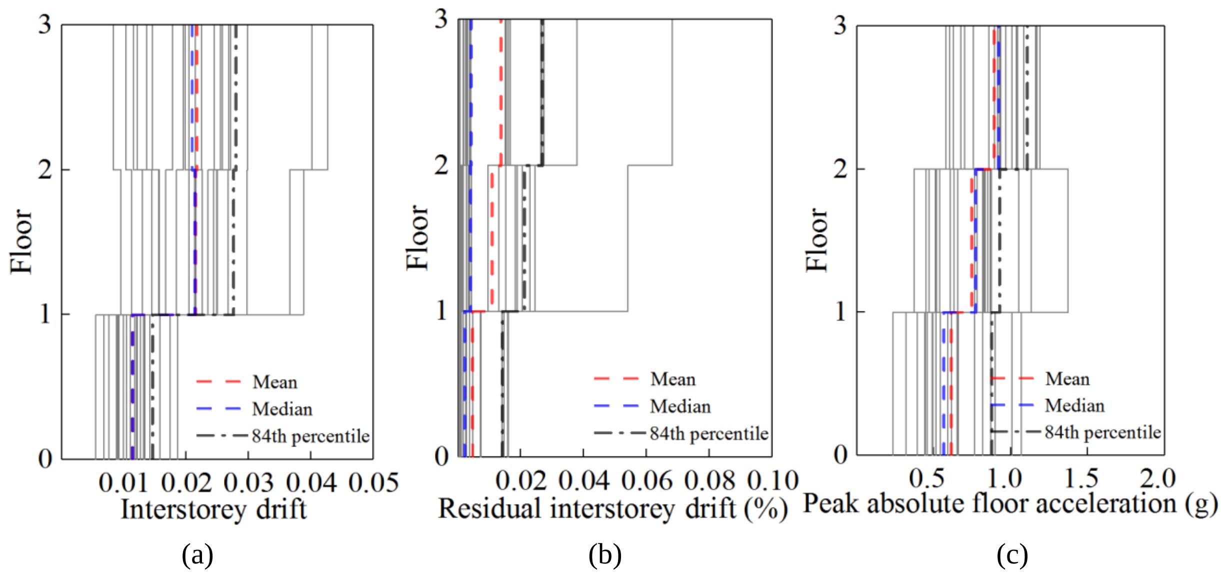

Fig. 7 – Seismic reponses: (a) Maximum interstorey drifts, (b) Residual interstorey drifts, (c) Peak absolute floor acceleration.

Although the MID responses are generally above 2%, the RID responses are insignificant. In particular, the maximum RID responses of the prototype structure are below 0.1%, and the average RID response is generally below 0.03%. In contrast, the RID responses of conventional steel moment resisting frames (MRFs) under ground motions may exceed 0.5% [17]. Thus, the excellent self-centring behaviour of HSSF-SCEDB is confirmed.

The PA responses of the prototype structure are not exactly the same as the deformation responses (e.g. the prototype structure undergoes the most intense peak absolute floor acceleration response when subjected to ground motion LA19), although a large deformation response is usually accompanied with a large PA response. This finding is understandable because the PA response is generally associated with multiple factors, such as the first period of vibration, number of stories of the structure, selection of the ground motion, and nonlinear behaviour of the structure [18].

Fig 8 shows the ratio of plastic energy dissipation of the main frames and the entire structure under ground motions. It can be seen that the ratios of plastic energy dissipation of the main frames and the entire structure under ground motions are generally insignificant. It means that SCEDBs are the primary source of hysteretic energy dissipation, and the main frames are slightly damaged or even damage-free under the input ground motions.

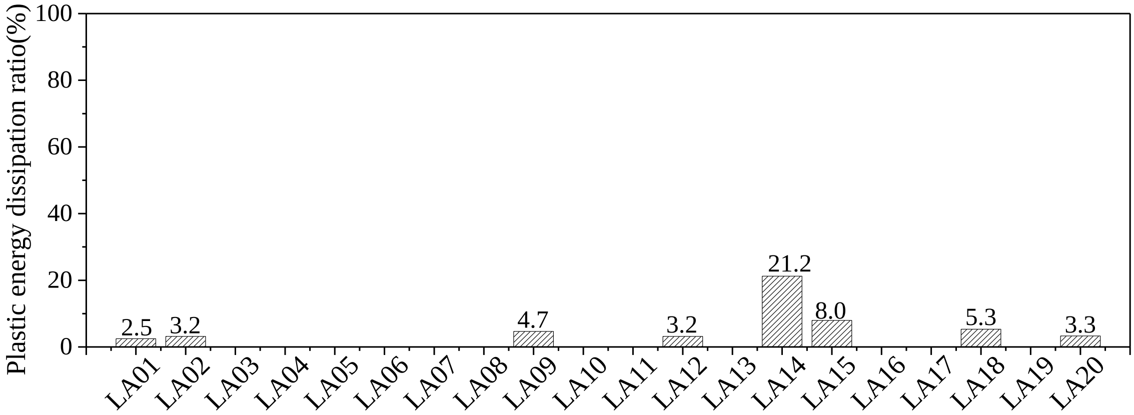

Fig. 8 – Ratio of plastic energy dissipation of the main frames and the entire structure under ground motions.

4. Conclusions

The current conference paper presents a pilot study on the HSSF-SCEDBs, and the following conclusions can be obtained:

(1) The cyclic pushover result of the HSSF-SCEDB shows a typical flag-shape hysteretic response, excellent self-centring behaviour, moderate energy dissipation capacity, and damage-control behaviour for a wide inelastic deformation range.

(2) The NL-RHA results of the HSSF-SCEDBs show that the maximum interstorey drift responses are associated with the spectral acceleration of the first mode period. The HSSF-SCEDB exhibits excellent self-centring behaviour with negligible post-earthquake residual interstorey drift even the maximum interstorey drift beyond the codified deformation threshold (i.e. 2%). The PA responses of the prototype structure are not exactly the same as the deformation responses.

(3) The SCEDBs are the primary source of hysteretic energy dissipation, and the main frames are slightly damaged even damage-free in the expected deformation range.

However, the current conference paper focuses on the effectiveness of HSSF-SCEDB in seismic performance, and not generates optimized structures. A more comprehensive study on the HSSF-SCEDBs is being conducted by the authors.

5. Acknowledgements

This research is financially supported by the National Natural Science Foundation of China (Grant No. 51890902 and 51708197) and Chinese National Engineering Research Centre for Steel Construction, The Hong Kong Polytechnic University (Project No. 1-BBV4).

6. References

[1] CEN Eurocode 8. Design of structures for earthquake resistance. Part1: General Rules, Seismic Actions and Rules for Buildings. European Committee for Standardization; 2004.

[2] Tremblay R, Bruneau M, Nakashima M, et al (1996): Seismic design of steel buildings: lessons from the 1995 Hyogo-ken Nanbu earthquake. *Canadian journal of civil engineering*, 23(3):727-756.

[3] Ke K, Chen Y (2016): Seismic performance of MRFs with high strength steel main frames and EDBs. *J Constr Steel Res;* 126:214-228.

[4] Chen Y, Ke K (2019): Seismic performance of high-strength-steel frame equipped with sacrificial beams of non-compact sections in energy dissipation bays. *Thin-Walled Struct*, 139:169-185.

[5] Ke K, Yam MCH, Deng L, Zhao Q (2018): A modified DEB procedure for estimating seismic demands of multi-mode-sensitive damage-control HSSF-EDBs. *J Constr Steel Res*, 150:329-345.

[6] Ke K, Wang W, Yam MCH, Deng L (2019): Residual displacement ratio demand of oscillators representing HSSF-EDBs subjected to near-fault earthquake ground motions. *Eng Struct*, 191:598-610.

[7] McCormick J, Aburano H, Ikenaga M, Nakashima M (2008): Permissible residual deformation levels for building structures considering both safety and human elements. *Proc 14th world conf earthquake engineering*. Beijing: Seismological Press of China.

[8] Christopoulos C, Tremblay R, Kim HJ, Lacerte M (2008): Self-centering energy dissipative bracing system for the seismic resistance of structures: development and validation. *J Struct Eng*, 134(1):96–107.

[9] C. Fang, M.C.H. Yam, A.C.C. Lam, L.K. Xie (2014): Cyclic performance of extended end-plate connections equipped with shape memory alloy bolts, *J. Constr. Steel Res*, 94 122–136.

[10] GB50011-2010 (2010): Code for Seismic Design of Buildings (GB 50011-2010). Chinese Building Press, Beijing, China.

[11] GB5009-2012 (2012): Load code for Design of Buildings (GB5009-2012). Chinese Building Press, Beijing, China.

[12] ABAQUS Analysis User's Manual (2012). ABAQUS Standard, Version 6.12.

[13] Auricchio F, Coda A, Reali A, Urbano M (2009): SMA numerical modeling versus experimental results: parameter identification and model prediction capabilities. *J Mater Eng Perform*, 18(5-6):649-54.

[14] Fang C, Yam MCH, Chan TM, Wang W, Yang X, Lin X (2017): A study of hybrid self-centring connections equipped with shape memory alloy washers and bolts. *Eng Struct*, 164:155-168.

[15] Somerville P (1997): Development of ground motion time histories for phase 2 of the FEMA/SAC steel project, SAC Background Document SAC/BD-91/04. Sacramento, Calif: SAC Joint Venture.

[16] Vargas R, Bruneau M (2009): Experimental response of buildings designed with metallic structural fuses. II. J Struct Eng, 135(4):394-403.

[17] Erochko J, Christopoulos C, Tremblay R, Choi H (2011): Residual drift response of SMRFs and BRB frames in steel buildings Designed according to ASCE 7-05. *J Struct Eng*, 137(5):589-599.

[18] Ray-Chaudhuri S, Hutchinson TC (2011): Effect of nonlinearity of frame buildings on peak horizontal floor acceleration. *J Earthq Eng*, 15(1):124–42.